



Effect of resin cement elastic modulus on the biaxial flexural strength and structural reliability of an ultra-thin lithium disilicate glass–ceramic material

Ana Flávia Nunes Reis¹ · Alexandre Luiz Souto Borges¹ · Thais Cachuté Paradella¹ · Rita Adriana Souza da Silva de Assis¹ · Luiz Felipe Valandro² · Renata Marques de Melo¹

Received: 3 February 2022 / Accepted: 18 December 2022 / Published online: 28 December 2022
© The Author(s), under exclusive licence to Springer-Verlag GmbH Germany, part of Springer Nature 2022

Abstract

Objectives Photo- and dual-polymerized resin-based luting agent was evaluated for elastic moduli effects on ultra-thin lithium disilicate (LD) glass–ceramic strengthening, structural reliability, and stress distribution.

Materials and methods One hundred-sixty LD discs (IPS e.max CAD, Ivoclar/Vivadent) were produced in ultra-thin thicknesses (half with 0.3 mm and the other half with 0.5 mm). The ultra-thin ceramic disks were coated with two different cement types (Variolink Veneer — V and Panavia F 2.0 — P). Two positive control groups were tested following hydrofluoric (HF) acid etching (LDt3, LDt5) and two negative control groups were tested for untreated ceramic (LD 3, LD 5). Biaxial flexural strength (BFS), characteristic strength (σ_0) and Weibull modulus (m) were the response variables ($n=20$) at the ceramic/resin cement interface ($z=0$). Finite element analysis (FEA) was used to calculate maximum principal stress. Data were analyzed using two-way ANOVA, and Tukey's test. Scanning electron microscopy (SEM) was used to analyze the failed specimens using fractography and surface morphology.

Results The BFS of LD at either thickness was not affected by cement types, as also demonstrated by FEA. Structural reliability significantly improved in the positive control group (LDt5).

Conclusion The cementation of ultra-thin LD with a resin-cement of varying elastic moduli did not influence BFS. LD surface modification by HF acid-etching increased the reliability.

Clinical relevance Ultra-thin anterior veneer designs made from lithium disilicate have been widely proposed and the apparent success of LD ultra-thin veneers was not influenced by the cement choice in the current studies albeit the elastic moduli luting agents used were of similar values.

Keywords Resin cement · Glass ceramics · Fractography, Flexural strength · Weibull analysis · Finite element analysis

Introduction

Thin restorations, such as laminate veneers, are considered as a minimally invasive alternative type of restoration for good clinical outcomes [1–3]. Their most advantageous characteristic is minimal dental preparation, maintaining the enamel, and better adhesion of the enamel/cement and cement/ceramic interfaces [4]. One of the most popular materials currently used for such restorations is lithium disilicate (LD) glass–ceramics, which present favorable mechanical properties when compared to traditional feldspathic and leucite ceramics [5], in addition to presenting translucency, surface gloss and light dispersion [6]. LD glass–ceramics materials also present high strength values to be used in veneer restorations of thin thicknesses [3, 7–9], such as those

✉ Ana Flávia Nunes Reis
dra-anaflavia@uol.com.br

¹ Institute of Science and Technology at São José Dos Campos, Department of Dental Materials and Prosthodontics, Univ. Estadual Paulista (UNESP), Eng. Francisco José Longo Avenue 777 - Jardim São Dimas, São José Dos Campos, SP 12245-000, Brazil

² Prosthodontics Unit, Post-Graduate Program in Oral Science, Federal University of Santa Maria, Santa Maria, Rio Grande Do Sul, Brazil

used in the treatment of occlusal abrasion or mis-positioned teeth [10].

In thin or ultra-thin restorations, the reduction in the proportion between ceramic and cement agent thicknesses can influence the veneers' stress distribution and longevity [11, 12]. The thinner the material, the higher the bending, leading to the increase of tensile stresses on the ceramic, which may lead to fracture [13]. In spite of that, previous studies have shown that ceramic fracture may also occur due to the polymerization shrinkage of the cement [14], the substrate type [15] and ceramic thickness [16]. Concerning thin restoration, the elastic modulus of the resin cement plays an important role in supporting the load generated by masticatory forces and dissipating it to the dental tissue [13]. The elastic modulus is a measure of the material's ability to resist elastic deformation under load, it makes an excellent measure of a luting materials capacity to transfer a load to a tooth and allow for stress distribution. Therefore, the resin cement absorbs stress [16, 17] and must present an intermediate elastic modulus value, between dentin and the restorative material [18–20] for stress distribution.

The mechanism of cement layer elastic modulus influence on ceramics has been widely explored [21–25]. The authors observed that an increase in the cement elastic modulus can act as a stress sink, causing a positive effect on ceramics. However, when considering different restorative material elastic modulus, the variation between ceramic thickness and flexural strength should be carefully evaluated to improve clinical performance [21].

The effect of a dual or light-curing resin cement concerning thin ceramic's inability to deform when subjected to masticatory stress is poorly understood. Thus, besides an examination of the mechanical properties of the materials involved, because each cement has its own chemical composition, the combination of an ultra-thin thickness with cements of different activation modes indicated for the same clinical conditions needs to be addressed. In reality, previous studies have addressed the problem of varying elastic moduli [21–24, 26], but this concern in clinics could be better translated into whether both the dual and photo polymerized cements can provide strong restorations. From these standpoints, one clinically relevant question needs to be answered: Can cements with distinct elastic modulus (dual and light-cured modes) and different composition affect the mechanical behavior of bonded LD glass–ceramic at ultra-thin thicknesses?

Finite element analysis (FEA) has been widely used as a mathematical solution to evaluate stress distribution and to determine stress peaks on the ceramic or the cement [13, 20, 27]. With this mechanical tool, it is possible to isolate structures and investigate the biomechanical behavior in different conditions. This study aimed to evaluate the influence of resin cement elastic modulus on the flexural

strength, structural reliability, and stress distribution of simplified LD ceramic restorations at 0.3 and 0.5 mm thickness. The hypothesis tested was that the higher the resin cement elastic modulus/moduli and the thicker the ceramic, the higher the flexural strength.

Material and methods

Specimens preparation

Lithium disilicate (LD) blocks (12 × 14 × 18 mm) (IPS e.max CAD, Ivoclar Vivadent, Shaan, Liechtenstein) were rounded by hand to produce a 12 mm diameter cylinder using a silicon carbide (SiC) abrasive paper (#280, #400, #600 #1200) in a polishing machine (EcoMet/AutoMet250, Buehler, USA) under copious water lubrication. The cylinders were sectioned to produce discs of 0.5 or 0.3 mm thickness using a low-speed diamond impregnated saw (Isomet 1000, Buehler, Lake Bluff, Illinois, USA) under constant water cooling. The discs were manually polished using SiC abrasive (#600, #800 and #1200) papers (Struers, Glasgow, UK) for 60 s until achieving the final thickness of 0.3 ± 0.1 mm ($n = 80$) or 0.5 ± 0.1 mm ($n = 80$) measured using a digital micrometer (Mitutoyo Corporation, Tokyo, Japan) with an accuracy of to 0.001 mm.

All discs were cleaned in an ultrasonic bath with distilled water and crystallized according to the manufacturer's instructions. The discs were placed on a crystallization tray (groups of six each time) and the firing cycles were conducted in a Programat EP 5000 (Ivoclar Vivadent, Shaan, Liechtenstein), using the following programme: Stand by temperature: 403 °C; Closing time: 6 min; Heating rate: 90 °C/30 °C; Firing temperature varying from 820 to 840 °C; Holding time: 10 s to 7 min; Vacuum: 550 °C/820 °C; Vacuum off: 840 °C; Cooling: 700 °C to room temperature.

Two resin cements were chosen for the specimen cementation in this study. The variation in elastic modulus and curing mode were the criteria for the resin cement selection. The cements were Variolink Veneer (Ivoclar Vivadent, Shaan, Liechtenstein) and Panavia F (Kuraray, Osaka, Japan). A total of 160 ultra-thin ceramic discs were produced and randomly distributed into the eight groups ($n = 20$): Variolink Vener (V), Panavia F (P), negative control (LD) positive control (LDt). Materials information are summarized in Table 1, although the elastic moduli of the two cements were provided by the manufacturers. Subsequently the elastic moduli were determined experimentally using a non-destructive and dynamic device, based on the impulse excitation technique.

Table 1 Brand name, manufacturer, composition, filler weight (wt.%) and volume (vol.%), elastic modulus (GPa) and the Poisson ratio of the cements used

Brand name	Manufacturer	Composition	Filler loading	Elastic modulus (GPa)	Poisson ratio
Panavia F 2.0	Kuraray, Osaka, Japan	Paste A: 10Methacryloyloxydecyl dihydrogen phosphate (MDP), hydrophobic aromatic dimethacrylate, hydrophobic aliphatic methacrylate, hydrophilic aliphatic dimethacrylate, silanated silica filler, silanated colloidal silica, DL-camphorquinone, catalysts, initiators, others Paste B: Sodium fluoride, hydrophobic aromatic dimethacrylate, hydrophobic aliphatic methacrylate, hydrophilic aliphatic dimethacrylate, silanated barium glass filler, catalysts, accelerators, pigments, others	78 wt.% 59 vol.%	10.19 ± 0.6	0.30
Variolink Veneer	Ivoclar Vivadent, Schaan, Liechtenstein	Dimethacrylates, inorganic filler, Ytterbium Trifluoride, Catalysts and stabilizers, Pigments	60.1 wt.% 40 vol.%	8.33 ± 0.9	0.30

Elastic modulus

To investigate the resin cements elastic moduli, three excitations were used to determine the flexional frequency. The pastes of Panavia were manually homogenized, then both cements were placed in a rectangular silicon matrix, light-irradiated with a light-emitting-diode (LED) light curing unit (LCU) operating at 1100 mW/cm² (Radii Plus, SDI Ltd., Bayswater, Victoria, Austrália) for 60 s at three points along the bar for a total irradiation time of 180 s. For these methods, bar-shaped specimens were cut and polished (#600 and #1200) until the final dimensions of: 40 × 10 × 2 mm. The bars ($n=2$) were positioned on Sonelastic® (Atcp Engenharia Física, São Carlos, Brazil), a non-destructive, dynamic device, based on the impulse excitation technique. The bars were weighed on an analytical scale (Shimadzu AY220) and measured with a digital pachymeter (Mitutoyo) and the data were inserted in the system's software. The Sonelastic® uses the sound emitted by the specimen when receiving a low mechanical stimulation, generating an acoustic response through natural vibration frequency proportional to the elastic modulus of the material (ASTM E1876-09) [28]. The Poisson ratio, the ratio between axial and transverse deformations, that is a necessary property for the FEA was also calculated by the software.

Surface treatment and cementation

Groups ($n=20$) were distributed according to the ceramic thickness (0.3 or 0.5 mm) and cement elastic modulus. For the resin luted specimens, prior to cementation, the ceramic bonding surfaces were treated with 5% hydrofluoric (HF) acid etch (Fórmula & Ação, São Paulo, Brazil) for 20 s,

rinsed with distilled water for 40 s and air-dried with oil-free compressed air for 60 s. In sequence, the specimens were silane treated (Monobond N, Ivoclar-Vivadent, Schaan, Liechtenstein), a thin coat of Monobond N was applied with a microbrush to the surfaces of the pre-treated discs, the material was allowed to react for 60 s; subsequently, it was dispersed to remove any remaining excess with a strong stream of air. Then, the groups were cemented according to the cementing agent: for Panavia F 2.0, the catalyst and base were manually mixed in equal proportions and applied onto the center of the treated ceramic disc. While for Variolink Veneer, the resin cement was directly applied to the treated surface. A mylar sheet, whose thickness was previously measured and discounted, was then compressed against the cement layer by the plates of a micrometer (Mitutoyo Corporation, Tokyo, Japan) that had been previously reset, to guarantee 100 µm thickness [29]. The excess of the cements was carefully removed from the sides of the specimen and the set was light irradiated laterally with the LED LCU for four points for 20 s from four different directions [29]. Further, 20 s irradiations were obtained after the specimen was removed from the micrometer to ensure the polymerization of the cement at the center of the disc and stored in distilled water at 37 °C for 24 h before testing and analysis.

Biaxial flexural strength (BFS)

For the BFS test (ISO 6872) [30], the specimens were placed in a circular metal base with three balls of 3.2 mm diameter, equally distant from each other. The device for testing was placed in the universal testing machine (Emic DL-1000, Emic, São José dos Pinhais, PR, Brazil), aligned with respect to the piston to ensure that the loading was symmetrical and

concentric. During the flexural test, the assembly was put in distilled water at a constant temperature of 37 °C. A flat tungsten piston ($\varnothing = 1.6$ mm) was used to apply an axial load at a crosshead speed (1.0 mm/min) until ceramic fracture, the load for the fracture of the sample was recorded. According to the guidelines of ISO (6872) [30], the BFS (MPa) of the specimens from the control group monolayers (no cement layer) was calculated according to the following equation:

$$\sigma = -0.2387P \frac{(X - Y)}{b^2} \quad (1)$$

where σ is the maximum tensile stress P is the total at fracture (N), X is the Poisson ratio, Y the elastic properties of the material and b is the specimen thickness at fracture origin.

For cemented samples, the biaxial stress was calculated according to analytical solutions described and tested by Hsueh et al. (2006) [31]. Thus, the BFS of the bilayered luted specimens was calculated at the central z -axis positions, where $z = 0$ was the ceramic/resin cement interface, and $z = -t_2$ was the point at which the tip of the device touches the resin cement, as can be seen in the following equations, respectively:

$$\sigma_1 = \frac{-E_1(z-z^*)P}{8\pi(1-\nu_1)D^*} \left\{ 1 + 2 \ln \left(\frac{a}{c} \right) + \frac{1-\nu}{1+\nu} \left[1 - \frac{c^2}{2a^2} \right] \frac{a^2}{R^2} \right\} \quad (2)$$

In which σ^1 is true for ($0 \leq z \leq t_1$ and $r \leq c$).

$$\sigma_2 = \frac{-E_2(z-z^*)P}{8\pi(1-\nu_2)D^*} \left\{ 1 + 2 \ln \left(\frac{a}{c} \right) + \frac{1-\nu}{1+\nu} \left[1 - \frac{c^2}{2a^2} \right] \frac{a^2}{R^2} \right\} \quad (3)$$

In which σ^2 is true for ($t_1 \leq z \leq t_1$ and $r \leq c$). P is the maximum load to fracture, a is the radius of the supporting circle, c is the piston radius, R is the specimen radius, r is the distance on the x -axis of the center of the disk, and z is the positioning of the interface on the y -axis.

Besides those, z^* (Eq. (3)), D^* (Eq. (4)) and ν (Eq. (5)), respectively corresponding to the neutral plane, the rigidity under flexure and the Poisson ratio of the bilayered specimens were determined.

$$z^* = \frac{\frac{E_1 t_1^2}{2(1-\nu_1^2)} + \frac{E_2 t_1^2}{2(1-\nu_2^2)} + E_2 t_1 t_2 / (1 - \nu_2^2)}{\frac{E_1 t_1^2}{(1-\nu_1^2)} + \frac{E_2 t_2^2}{(1-\nu_2^2)}} \quad (4)$$

$$D^* = \frac{E_1 t_1^3}{3(1-\nu_1^2)} + \frac{E_2 t_2^3}{3(1-\nu_2^2)} + \frac{E_2 t_1 t_2 (t_1 + t_2)}{1 - \nu_2^2} \frac{\left[\frac{E_1 t_1^2}{2(1-\nu_1^2)} + \frac{E_2 t_2^2}{2(1-\nu_2^2)} + E_2 t_1 t_2 / (1 - \nu_2^2) \right]^2}{\frac{E_1 t_1}{(1-\nu_1^2)} + E_2 t_2 / (1 - \nu_2^2)} \quad (5)$$

$$\nu = \frac{\nu_1 t_1 + \nu_2 t_2}{t_1 + t_2} \quad (6)$$

The elastic modulus (E_1) and Poisson ratio (ν_1) of the LD glass ceramic and resin cement (E_2 and ν_2) were previously calculated (Table 1). In addition, t_1 represents the ceramic thickness, while t_2 represents the resin cement thickness.

The BFS data were then checked for homoscedasticity and analyzed through a two-way ANOVA (cement \times ceramic thickness), and paired Tukey test ($\alpha = 5\%$). (*MINITAB for Windows*, version 17, *Minitab, Inc.*). In addition, Weibull analysis [32] was used to evaluate for a calculation of failure probabilities using maximum likelihood estimation, in which the overlapping of confidence intervals (IC = 95%) represented no statistically significant differences between groups.

Finite element analysis (FEA)

The experimental conditions were also analyzed through FEA. The models were created using a modeling software (Rhinoceros 5.0—McNeel North America, Seattle, WA, USA), according to the experimental setup (Fig. 2) and exported in *STEP* format for the structural analysis.

Structural static analysis was performed using Ansys 19R2 (ANSYS Inc, Houston, TX, USA) software. The mechanical properties of Elastic modulus (GPa) and Poisson ratio for Stainless steel and IPS Emax CAD were 210 GPa, 0.30 (ANSYS Database), and 95 GPa, 0.23 (Ivoclar/Vivadent), respectively. For the cements under study (Panavia F 2.0 and Variolink Veneer), these values were obtained using the Sonelastic device (Atpc Engenharia Física, São Carlos, Brazil), as previously described. All materials were considered elastic, isotropic, and homogenous.

The contact between cement and ceramic was considered perfectly bonded whereas, between the cement and the metal base, a coefficient of friction of 0.12 was assumed. The models consisted of tetrahedral elements, resulting in a total of 280,464 elements and 750,702 nodes, for the 0.5 mm thick ceramic and 294,877 elements and 530,640 nodes for the 0.3 mm thick ceramic.

The discs were loaded a 75 N load, using a similar tip used in experimental test, compressing a 0.44 mm² area of the top of ceramic, and constrained in three axes at the base of three spheres. A static structural analysis was performed, and the maximum principal stress was considered as failure criteria, as usually chosen to brittle materials analysis.

Mode of failure analysis

All failed samples were analyzed under stereomicroscopy (Discovery V20, Carl-Zeiss, Gottingen, Germany) and Scanning Electron Microscopy for failure origin inspection.

Samples were gold-sputtered and inspected under SEM (Inspect S50, FEI—Tchec Republic) imaging with different magnifications using a secondary electron detector (ETD).

Results

Elastic modulus

The mechanical properties of Elastic modulus (GPa) of the two cements analyzed were 8.33 ± 0.9 for Variolink Veneer, and 10.19 ± 0.6 for Panavia F 2.0.

Biaxial flexural strength (BFS) and Weibull statistical analysis

The results are presented in Table 2 for ceramic discs (coated and without coating) in two thicknesses of 0.3 and 0.5 with confidence intervals (CI) of 95%. For the bilayered specimens, the values considered were at $Z=0$ (the ceramic/resin cement interface).

For the BFS data, a two-way ANOVA revealed that the type of treatment was associated with ceramic strength ($p=0.000$), but the ceramic thickness did not ($p=0.214$). It was observed that thickness and treatment interacted significantly to influence specimen behavior ($p=0.004$).

The mean BFS of disc samples tested no-acid etching (Negative control) LD3 was 412.37 ± 90.94 MPa and significantly different from the thicker unetched group (LD5) also from positive control groups (LDt3, LDt5) (Table 2). A notable improvement in mechanical reliability (m) of 15.77 ± 11.24 was observed in the positive control group LDt3, although flexural strength was not significantly different when compared to the thicker positive control group LDt5.

Regarding the cemented groups (V5, V3, P5, P3), a significant decrease of the flexural strength in all groups compared with control groups was observed. The P3 group had the lowest biaxial flexural strength numerically (σ). The 95%

confidence intervals of the Weibull moduli overlapped, indicating that the reliability of fracture strength data was not significant for cemented groups. Figure 1 shows the Weibull graph for all groups.

FEA

Schematic illustrations of the specimens of 3-D FEA replicating the BFS test are represented in Fig. 2. Compressive (negative) stresses were noticed at the ceramic surface in contact with the supports for the flexural testing. Higher tensile (positive) stress concentration occurred on the surfaces of the ceramic and cement agent that face the bottom ring (on the center of all the samples), as expected in this type of testing. The ceramic thickness was the main factor affecting the stresses distribution numerically. The maximum principal stresses observed were in the thinner groups (LD3/V3/P3). For the cement factor, the difference was less than 10%. Figure 2 shows that stress distribution (StD) was concentrated in the center of samples, below load point and the maximal principal stress peak (MPSp) and StD at the tension ceramic surface.

Both MPSp and StD were higher to 0.3 mm than 0.5 mm with or without cement. Although Variolink Veneer has shown MPSp numerically higher than Panavia F 2.0, the values were less than the values obtained to mesh convergence.

FEA has not shown similarly in vitro behavior when both ceramic thicknesses were compared, the effect of the different elastic modulus of cements used was similar and unable to increase the flexural strength of samples.

Bullet Failure mode

Representative images of the SEM fractographic analysis are shown in Fig. 3. Failure was not induced by contact damage on the compressive surface. In the non-bonded specimens (control group), the failures started at the tensile side of the ceramic. For all bonded samples, the crack started from the defect at the tensile side of the ceramic, close to the interface

Table 2 Mean biaxial flexural strength (σ), characteristic strength (σ_0), and Weibull moduli (m) with Confidence Intervals (CI) of 95% of monolayers groups (LD3/LD5/LDt3/LDt5) and cemented groups (V3/V5/P3/P5) at Axial position $z=0$. Numbers in parentheses refer to standard deviations

Group	$\sigma \pm$ SD strength (MPa)	σ_0 (MPa)	m
Negative Control LD3	412.37 (90.94) ^A	447.95 (408.00–491.85) ^a	4.95 (3.60–6.85) ^A
Negative Control LD5	354.14 (78.06) ^B	383.95 (352.31–420.61) ^b	5.36 (3.74–7.67) ^B
Positive Control LDt3	336.00 (26.80) ^B	347.65 (337.62–357.96) ^c	15.77 (11.12–22.36) ^C
Positive Control LDt5	315.64 (33.27) ^{B,C}	329.46 (317.00–342.41) ^d	11.95 (8.51–16.79) ^D
V3	274.22 (46.81) ^{C,D}	294.01 (273.00–316.65) ^e	6.27 (4.52–8.68) ^E
V5	275.00 (51.88) ^{C,D}	296.05 (273.82–320.08) ^e	5.94 (4.26–8.27) ^E
P3	240.52 (38.05) ^D	256.34 (241.26–272.35) ^f	7.63 (5.37–10.84) ^E
P5	274.16 (50.35) ^{C,D}	293.84 (275.79–313.06) ^e	7.24 (5.00–10.47) ^E

^{A,C,B} Means and Standard deviation in rows followed by the different capital letters are considered statistically different from each other ($p > 0.05$). Distinct letters and symbols in each column indicate significant differences between groups

Fig. 1 Failure Probability (Weibull analysis) for all groups — LD3, LD5, LDt3, LDt5, V3, V5, P3, P5

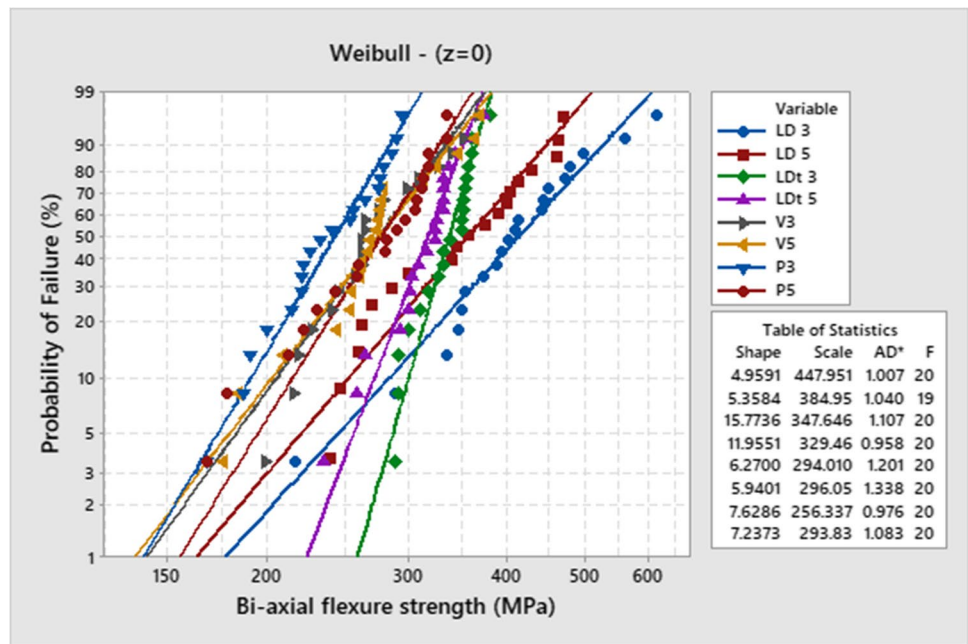
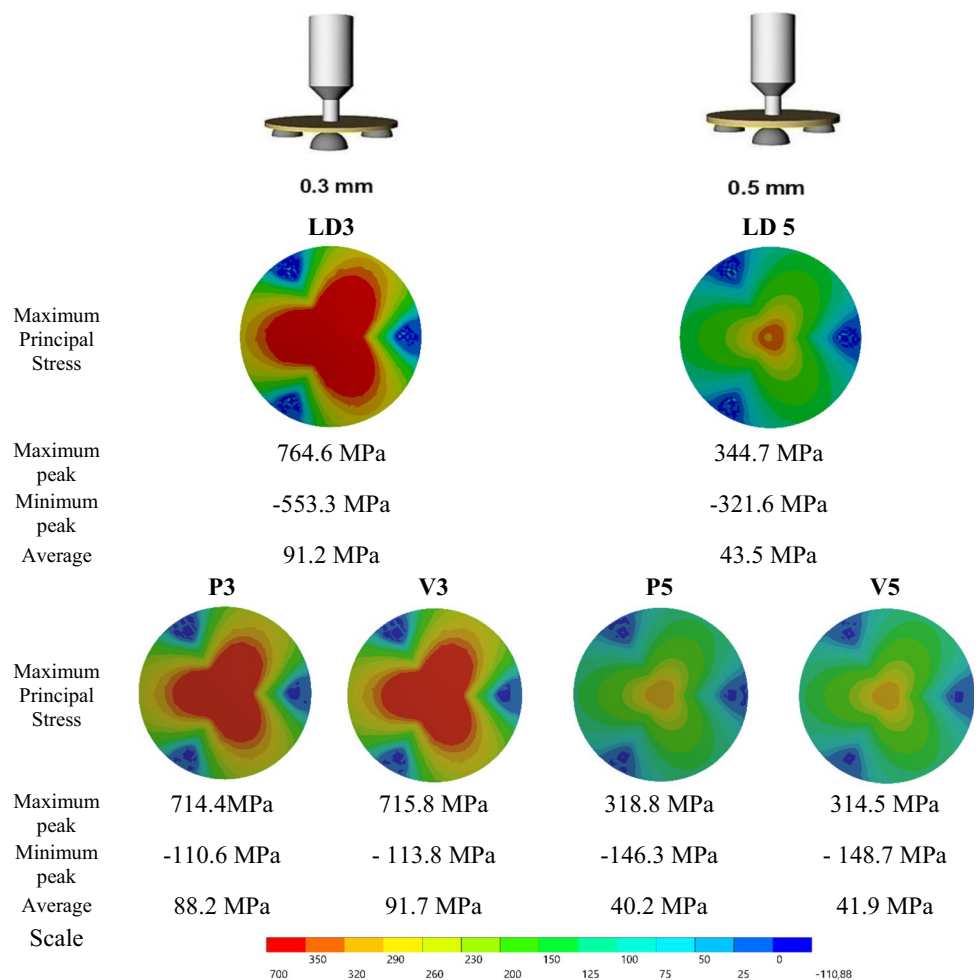


Fig. 2 Schematic illustration of the specimens positioned on the supports for the flexural testing. Under, colorimetric results for Maximum Principal Stress results in 0.3 mm and 0.5 mm non-cemented control groups (LD3/LD5) and cemented groups (V3/P3/V5/P5)



(Fig. 3). In most cases, the cements seemed to have filled up the irregularities of the ceramic surfaces; however, in the group with the higher elastic modulus (P3/P5), some gaps were found between the ceramic and the cementing agent layer (Fig. 3C).

Discussion

This study evaluated the influence of two resin cements with varying elastic moduli on the flexural strength, structural reliability, and stress distribution of LD ceramic restorations at two ultra-thin thicknesses.

Previous studies [21–24, 26] have demonstrated the effects of different resin cements with varying elastic moduli on the flexural strength of various ceramics. However, the main concern regarding the impact of cementation on ultra-thin ceramic thickness has hardly been addressed. Although thinner thicknesses are more prone to deflection, there is, to some extent, a compensation provided by high elastic modulus cements for preventing fractures [22]. It is also important to mention that the mode of activation of the cements in the present study was different, as well as their composition (microstructure and amount of inorganic load present in the resin matrix).

In Table 2, the mean BFS and associated standard deviation for the negative controls (polished surfaces) were higher for the 0.3 mm thick LD specimens compared with the more voluminous 0.5 mm disc-shaped specimens. This effect is a result of the increased likelihood for large defects to be included in the larger specimens in line with the weakest link in the chain concept proposed by Weibull in 1951 [32]. In addition, the positive control groups highlight a similar trend for increasing mean BFS and associated standard deviation for the 0.3 mm samples compared with the 0.5 mm thickness samples. The reduction in the mean BFS and associated standard deviation for the positive control compared with the negative control for all thicknesses was associated with the HF acid etching the glass in the LD restorative material manifest as increased surface tortuosity with the associated reduction in the mean BFS and associated standard deviation. Resin cementation would be expected to increase the mean BFS and associated standard deviation of the bilayered specimens. However, this effect was not observed in the current study possibly owing to delamination being evident following testing the bilayered specimens. A similar result was produced by Addison et al. [33] when applying resin-based luting agents to polished surfaces. It is proposed that a rougher interface would have allowed the resin-ceramic hybrid layer to become active and produce the expected increase in mean BFS and associated standard deviation indicative of resin luting LD ceramics.

In the present study, two commercially available resin cements with different composition were selected: Variolink Veneer which is free from adhesive monomers and Panavia which is a dual cement that contains the adhesive monomer 10-MDP. They behave, therefore, differently in water. After 24 h, there were no significant differences in BFS among the bilayer groups (V3, V5, P3, P5), suggesting that the greatest difference should occur immediately after curing, but these differences tend to disappear after storage in water (which may be due to residual polymerization or a plasticizing effect by water absorption) [34]. A thermal-cycling period was not used in the current investigation (all samples were kept in distilled water for 24 h before being tested), although the samples coated with Panavia F (P3/P5) seemed to present early hydrolytic susceptibility [35].

In addition, to the profound effect of HF acid etching on the surface modification of glass ceramics, a residence flow population has been shown to affect the fracture strength and reliability of thin laminate porcelain restorations [36]. Despite using a different glass ceramic (lithium disilicate) and HF at a low concentration (5%) in the current study, a statistically significant trend towards an increased Weibull modulus was observed in the uncoated/etched groups (LDt3/LDt5) showing that acid etching modified surface flaws. In contrast, the cemented groups (V3, V5, P3 and P5) showed a different pattern, suggesting that interpenetration of resin on the surface of the specimens did not affect crack healing as much as expected, showing a decrease for the structural reliability.

Regarding the thickness of the specimens, the present study showed that it did not statistically influence the BFS of cemented groups (Table 2), agreeing with results highlighted by De Angelis et al. [3]. These findings contradict the results obtained by Ge et al. [16] and Sasse et al. [10], in which the groups with higher thickness presented higher resistance, adding to the fact that the thicker groups adhered to dentin also presented superior results when compared to thinner groups. When one considers the non-cemented specimens, however, a lower BFS of thicker specimens was observed, which agrees with the idea that an increase in the volume of the specimen increases the number of possible defects and affects the structural homogeneity Weibull modulus of the material (Table 2).

When the experimental conditions were evaluated through FEA, it was observed that with a load of 75 N, the maximum principal stress values of the cement with the lower elastic modulus (Variolink Veneer) were numerically superior (Fig. 2). From this standpoint, it can be affirmed that the stresses concentrated in the cement layer were numerically higher and reduced the stresses transmitted to the ceramic. However, FEA revealed no significant difference in the flexural strength when varying the resin cement, which corroborated the laboratory results. Thus,

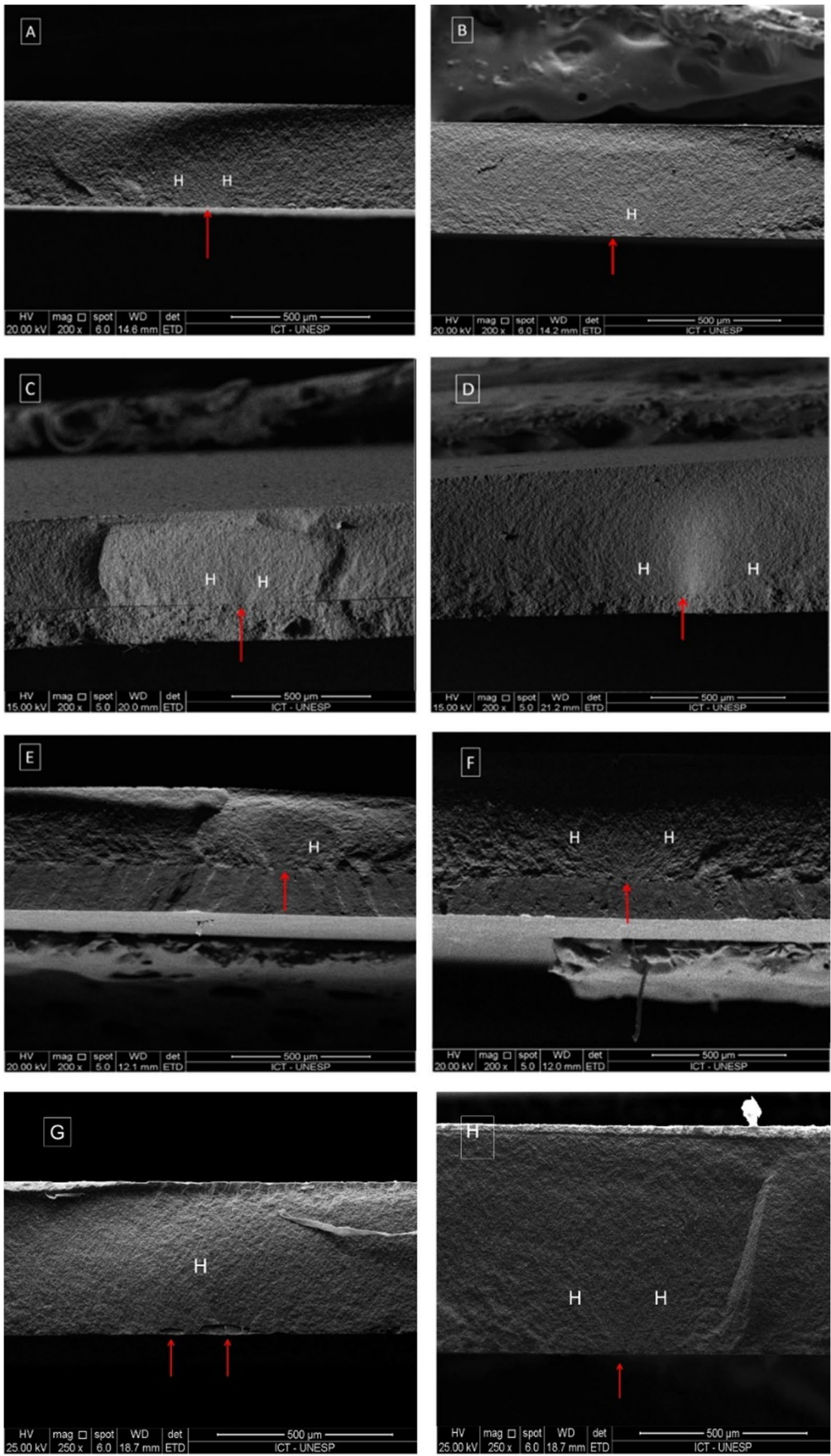


Fig. 3 SEM images of fractured surfaces for all groups tested (A) LD 3, (B) LD 5 (C) P3; (D) P 5, (E) V3, (F) V5, (G) LDt3, (H) LDt5 respectively, where the arrows show the fracture origin and letter H represents Hackles. In all bilayer groups, the origin of the fractures was in the ceramic

other factors, such as the cement filling of the defects on the ceramic surface and even the shrinkage of the cement (which may favor the healing of cracks) could account for the difference found in other studies because the materials were considered without defects. Therefore, future studies should address the evaluation of other cement and ceramics (at various thicknesses) in thin restorations, especially ones tailored to receive higher masticatory loads in posterior teeth.

Failure origin can vary depending on sample geometry, stress circumstances, and material characteristics. This present study has analyzed the influence of the elastic modulus of the cement layer on the behavior of a restorative material (LD) in two ultra-thin thicknesses (0.3 and 0.5 mm). Fractography analysis provided additional insight into the description of varying elastic modulus of the cement, resulting in no difference in the cemented groups. Even when testing cement agents with higher elastic modulus, the failure origin was located at the ceramic structure of the bilayer's samples rather than at the cement layer, different from what was expected. In this scenario, the load required for fracture was not increased, consequently, the stresses towards the LD have not been difficult in finding flaws to initiate the crack; it seems that the cement with higher (E) did not evenly fill up the etched ceramic surface.

Limitations of the present study are the absence of long-term and thermal cycling aging for bond degradation (bond hydrolysis), the use of a simplified model to mimic posterior restorations (disc-disc set-up), and the absence of sliding movement during cyclic loading application.

Conclusion

Despite the limitations of this study, it was concluded that resin cements of varying elastic moduli, photo- or dual-polymerized, did not lead to increased BFS of LD glass-ceramic on ultra-thin thicknesses albeit the elastic moduli employed differed by only 10% (8.33 ± 0.9 for Variolink Veneer, and 10.19 ± 0.6 for Panavia F 2.0). A significant increase in the structural reliability (Weibull modulus) of an ultra-thin LD ceramic has been demonstrated from HF acid-etching, showing that greater influence exists of surface flaw modification after HF acid-etching. Based on the observed failure modes, the crack origin was always on the ceramic tensile surface.

Author contribution Ana Flávia Nunes Reis, Alexandre Luiz Souto Borges, Thais Paradella, Rita Adriana Souza da Silva de Assis, Luiz Felipe Valandro, Renata Marques de Melo contributed equally to this work.

Funding This work was supported by Coordination for the Improvement of Higher Education Personnel (CAPES).

Declarations

Competing interests The authors declare no competing interests.

References

1. Peumans M, Van Meerbeek B, Lambrechts P, Vanherle G (2000) Porcelain veneers: a review of the literature. *J Dent* 28(3):163–177. [https://doi.org/10.1016/s0300-5712\(99\)00066-4](https://doi.org/10.1016/s0300-5712(99)00066-4)
2. Okida RC, Filho AJ, Barao VA, Dos Santos DM, Goiato MC (2012) The use of fragments of thin veneers as a restorative therapy for anterior teeth disharmony: a case report with 3 years of follow-up. *J Contemp Dent Pract* 13(3):416–420. <https://doi.org/10.5005/jp-journals-10024-1160>
3. De Angelis F, D'Arcangelo C, Vadini M (2021) The effect of dentin bonding and material thickness on the flexural properties of a lithium-disilicate glass-ceramic. *J Adhes Dent* 23(4):309–318. <https://doi.org/10.3290/j.jad.b1650013>
4. Rotoli BT, Lima DA, Pini NP, Aguiar FH, Pereira GD, Paulillo LA (2013) Porcelain veneers as an alternative for esthetic treatment: clinical report. *Oper Dent* 38(5):459–466. <https://doi.org/10.2341/12-382-T>
5. Guess PC, Zavanelli RA, Silva NR, Bonfante EA, Coelho PG et al (2010) Monolithic CAD/CAM lithium disilicate versus veneered Y-TZP crowns: comparison of failure modes and reliability after fatigue. *Int J Prosthodont* 23(5):434–442
6. Höland W, Rheinberger V, Wegner S, Frank M (2000) Needle-like apatite-leucite glass-ceramic as a base material for the veneering of metal restorations in dentistry. *J Mater Sci Mater Med* 11(1):11–17. <https://doi.org/10.1023/a:1008977416834>
7. Raigrodski AJ (2004) Contemporary materials and technologies for all-ceramic fixed partial dentures: a review of the literature. *J Prosthet Dent* 92(6):557–562. <https://doi.org/10.1016/j.prosdent.2004.09.015>
8. Conrad HJ, Seong WJ, Pesun IJ (2007) Current ceramic materials and systems with clinical recommendations: a systematic review. *J Prosthet Dent* 98(5):389–404. [https://doi.org/10.1016/S0022-3913\(07\)60124-3](https://doi.org/10.1016/S0022-3913(07)60124-3)
9. Della Bona A, Kelly JR (2008) The clinical success of all-ceramic restorations. *J Am Dent Assoc* 139:8S–13S. <https://doi.org/10.14219/jada.archive.2008.0361>
10. Sasse M, Krummel A, Klosa K, Kern M (2015) Influence of restoration thickness and dental bonding surface on the fracture resistance of full-coverage occlusal veneers made from lithium disilicate ceramic. *Dent Mater* 31(8):907–915. <https://doi.org/10.1016/j.dental.2015.04.017>
11. Blatz MB, Sadan A, Martin J, Lang B (2004) In vitro evaluation of shear bond strengths of resin to densely sintered high-purity zirconium-oxide ceramic after long-term storage and thermal cycling. *J Prosthet Dent* 91(4):356–362. <https://doi.org/10.1016/j.prosdent.2004.02.001>
12. Öztürk E, Chiang YC, Coşgun E, Bolay Ş, Hickel R, Ilie N (2013) Effect of resin shades on opacity of ceramic veneers and polymerization efficiency through ceramics. *J Dent* 41(Suppl 5):e8–e14. <https://doi.org/10.1016/j.jdent.2013.06.001>

13. Tribst JPM, Dal Piva AMO, Penteadó MM, Borges ALS, Bottino MA (2018) Influence of ceramic material, thickness of restoration and cement layer on stress distribution of occlusal veneers. *Braz Oral Res* 32:e118. <https://doi.org/10.1590/1807-3107bor-2018.vol32.0118>
14. Magne P, Versluis A, Douglas WH (1999) Effect of luting composite shrinkage and thermal loads on the stress distribution in porcelain laminate veneers. *J Prosthet Dent* 81(3):335–344. [https://doi.org/10.1016/s0022-3913\(99\)70278-7](https://doi.org/10.1016/s0022-3913(99)70278-7)
15. Ge C, Green CC, Sederstrom DA, McLaren EA, Chalfant JA, White SN (2018) Effect of tooth substrate and porcelain thickness on porcelain veneer failure loads in vitro. *J Prosthet Dent* 120(1):85–91. <https://doi.org/10.1016/j.prosdent.2017.10.018>
16. Ge C, Green CC, Sederstrom D, McLaren EA, White SN (2014) Effect of porcelain and enamel thickness on porcelain veneer failure loads in vitro. *J Prosthet Dent* 111(5):380–387. <https://doi.org/10.1016/j.prosdent.2013.09.025>
17. Zarone F, Apicella D, Sorrentino R (2005) Influence of tooth preparation design on the stress distribution in maxillary central incisors restored by means of alumina porcelain veneers: a 3D-finite element analysis. *Dent Mater* 21(12):1178–1188. <https://doi.org/10.1016/j.dental.2005.02.014>
18. Li ZC, White SN (1999) Mechanical properties of dental luting cements. *J Prosthet Dent* 81(5):597–609. [https://doi.org/10.1016/s0022-3913\(99\)70216-7](https://doi.org/10.1016/s0022-3913(99)70216-7)
19. Furuichi T, Takamizawa T, Tsujimoto A, Miyazaki M, Barkmeier WW, Latta MA (2016) Mechanical properties and sliding-impact wear resistance of self-adhesive resin cements. *Oper Dent* 41(3):E83–E92. <https://doi.org/10.2341/15-033-L>
20. Penteadó MM, Mendes Tribst JP, Dal Piva AMO, Archangelo KC, Bottino MA, Souto Borges AL (2020) Influence of different restorative material and cement on the stress distribution of ceramic veneer in upper central incisor. *Indian J Dent Res* 31(2):236–240. https://doi.org/10.4103/ijdr.IJDR_150_18
21. Fleming GJP, Hooi P, Addison O (2012) The influence of resin flexural modulus on the magnitude of ceramic strengthening. *Dent Mater* 28(7):769–776. <https://doi.org/10.1016/j.dental.2012.04.003>
22. Spazzin AO, Guarda GB, Oliveira-Ogliari A, Leal FB, Correr-Sobrinho L, Moraes RR (2016) Strengthening of porcelain provided by resin cements and flowable composites. *Oper Dent* 41(2):179–188. <https://doi.org/10.2341/15-025-L>
23. Spazzin AO, Bacchi A, Alessandretti R, Santos MB, Basso GR, Griggs J, Moraes RR (2017) Ceramic strengthening by tuning the elastic moduli of resin-based luting agents. *Dental Mater* 33(3):358–366. <https://doi.org/10.1016/j.dental.2017.01.002>
24. Penteadó MM, Tribst JPM, Jurema ALB, Saavedra GSFA, Borges ALS (2019) Influence of resin cement rigidity on the stress distribution of resin-bonded fixed partial dentures. *Comput Methods Biomech Biomed Engin* 22(10):953–960. <https://doi.org/10.1080/10255842.2019.1609456>
25. Assaf J, Hardan L, Kassis C, Bourgi R, Devoto W, Amm E, Moussa C, Sawicki J, Lukomska-Szymanska M (2021) Influence of resin cement thickness and elastic modulus on the stress distribution of zirconium dioxide inlay-bridge: 3D finite element analysis. *Polymers* 13(22):3863. <https://doi.org/10.3390/polym13223863>
26. Costa AK, Borges AL, Fleming GJP, Addison O (2014) The strength of sintered and adhesively bonded zirconia/veneering ceramic bilayers. *J Dent* 42(10):1269–1276. <https://doi.org/10.1016/j.jdent.2014.08.001>
27. Dal Piva AMO, Tribst JPM, Benalcázar Jalkh EB (2021) Minimal tooth preparation for posterior monolithic ceramic crowns: effect on the mechanical behavior, reliability, and translucency. *Dental Mater* 37(3):e140–e150. <https://doi.org/10.1016/j.dental.2020.11.001>
28. ASTM E1876 (2015) Standard test method for dynamic Young's modulus, shear modulus and Poisson's ratio by impulse excitation of vibration; ASTM International: West Conshohocken, PA, USA
29. Salazar Marocho SM, de Melo RM, Macedo LG, Valandro LF (2011) Bottino MA (2011) Strength of a feldspar ceramic according to the thickness and polymerization mode of the resin cement coating. *Dent Mater J* 30(3):323–329. <https://doi.org/10.4012/dmj.2010-123>
30. International Organization for Standardization, D.C., 3rd ed. ISO; 2008. ISO 6872
31. Hsueh CH, Luttrell CR, Becher PF (2006) Modelling of bonded multilayered disks subjected to biaxial flexure tests. *Int J Solids Struct* 43:6014–6025. <https://doi.org/10.1016/j.ijsolstr.2005.07.020>
32. Weibull W (1951) A statistical distribution function of wide applicability. *J Appl Mech* 18:293–297
33. Addison O, Marquis PM, Fleming GJP (2008) Quantifying the strength of a resin-coated dental ceramic. *J Dent Res* 87(6):542–547. <https://doi.org/10.1177/154405910808700610>
34. Pace LL, Hummel SK, Marker VA, Bolouri A (2007) Comparison of the flexural strength of five adhesive resin cements. *J Prosthodont* 16(1):18–24. <https://doi.org/10.1111/j.1532-849X.2006.00151.x>
35. Tzanakakis EG, Dimitriadi M, Tzoutzas I, Koidis P, Zinelis S, Eliades G (2021) Effect of water storage on hardness and interfacial strength of resin composite luting agents bonded to surface-treated monolithic zirconia. *Dent J (Basel)* 9(7):78. <https://doi.org/10.3390/dj9070078>
36. Addison O, Marquis PM, Fleming GJP (2007) The impact of hydrofluoric acid surface treatments on the performance of a porcelain laminate restorative material. *Dent Mater* 23(4):461–468. <https://doi.org/10.1016/j.dental.2006.03.002>

Publisher's note Springer Nature remains neutral with regard to jurisdictional claims in published maps and institutional affiliations.

Springer Nature or its licensor (e.g. a society or other partner) holds exclusive rights to this article under a publishing agreement with the author(s) or other rightsholder(s); author self-archiving of the accepted manuscript version of this article is solely governed by the terms of such publishing agreement and applicable law.